POLITECNICO DI TORINO
Repository ISTITUZIONALE

A Wearable Brain-Computer Interface Instrument for Augmented Reality-Based Inspection in Industry 4.0

Original
A Wearable Brain-Computer Interface Instrument for Augmented Reality-Based Inspection in Industry 4.0 / Angrisani, L., Arpaia, P., Esposito, A., Moccaldi, N.. - In: IEEE TRANSACTIONS ON INSTRUMENTATION AND MEASUREMENT. - ISSN 0018-9456. - ELETTRONICO. - 69:4(2020), pp. 1530-1539. [10.1109/TIM.2019.2914712]

Availability:
This version is available at: 11583/2848080 since: 2020-10-10T15:23:42Z

Publisher:
Institute of Electrical and Electronics Engineers Inc.

Published
DOI:10.1109/TIM.2019.2914712

Terms of use:

This article is made available under terms and conditions as specified in the corresponding bibliographic description in the repository

Publisher copyright
IEEE postprint/Author's Accepted Manuscript

©2020 IEEE. Personal use of this material is permitted. Permission from IEEE must be obtained for all other uses, in any current or future media, including reprinting/republishing this material for advertising or promotional purposes, creating new collecting works, for resale or lists, or reuse of any copyrighted component of this work in other works.

(Article begins on next page)

09 November 2026

This article has been accepted for publication in a future issue of this journal, but has not been fully edited. Content may change prior to final publication. Citation information: DOI 10.1109/TIM.2019.2914712, IEEE Transactions on Instrumentation and Measurement

A Wearable Brain-Computer Interface Instrument for Augmented Reality-based Inspection in Industry 4.0

Leopoldo Angrisani[1], Pasquale Arpaia[1], Antonio Esposito[2] and Nicola Moccaldi[1]

***Abstract*—This paper proposes a wearable monitoring system for inspection in the framework of Industry 4.0. The instrument integrates Augmented Reality (AR) glasses with a non-invasive single-channel Brain Computer Interface (BCI), which replaces the classical input interface of AR platforms. Steady-state visually evoked potentials (SSVEP) are measured by a single-channel EEG and simple power spectral density analysis. The visual stimuli for SSVEP elicitation are provided by AR glasses while displaying the inspection information. The real-time metrological performance of the BCI is assessed by the Receiver Operating Characteristic curve on experimental data from twenty subjects. The characterization was carried out by considering stimulation times from 10.0 s down to 2.0 s. The thresholds for the classification were found to be dependent on the subject and the obtained average accuracy goes from 98.9% at 10.0 s to 81.1% at 2.0 s. An inspection case study of the integrated AR-BCI device show encouraging accuracy of about 80% of lab values.**

I. Introduction

Augmented Reality (AR) is a technology for overlapping computer-generated perceptual information with actual world, in order to enhance human perception of the surrounding environment [1], [2], [3]. In the last two decades, AR has gained great interest in the technical-scientific community and much effort has been done to overcome its limitations. D. Chatzopoulos et al. [4] provided a survey of mobile augmented reality regarding the applications, its main components, and the challenges to be faced nowadays. Mobile devices of concern are tablets, smartphones, and smart glasses (AR glasses). Typical user interfaces for these devices are touch screens, vocal commands, or gestures.

In an industrial context, the *Boston Consulting Group* identified Augmented Reality as one of the nine pillars of the ongoing industrial revolution, Industry 4.0 [5], [6]. AR can help several work aspects, from training on-the-job to product design, and maintenance [7], [8], [9]. According to a recent survey on more than 30 journal papers [9], the main maintenance operations where AR is used are training, inspections, diagnostics, assembly-disassembly, and repair. These operations usually require the user hands to be free from the AR device controller. Despite hands-held devices, such as tablets, smart glasses can guarantee hands-free operations with their high wearability, provided that their user input interface does not require hands.

The combination of AR with a Brain-Computer Interface (BCI) can provide the solution to a hands-free user input, thus providing a novel way of gathering information from the surrounding environment. BCI is a device capable of interpreting human intentions by reading user neuronal activity. Historically, most BCI researches focused on helping people with motor disabilities by providing an alternative communication channel [10], [11]. This is changing in the last decade, and BCI employment is now addressed to several application fields. Many paradigms have been developed for BCI systems, such as motor-imagery [12], [13], cognitive monitoring [14], P300 [15], or SSVEP [16], [17], [18]. Focusing on non-invasive electroencephalography (EEG), the brain activity is monitored as electrical signals measured on specific areas of the BCI user's scalp [19]. Each paradigm requires the extraction of specific features from a set of brain signals, such as a voltage peak or the frequency of an oscillation. Some studies have shown that SSVEPs are highly reliable in terms of accuracy and reproducibility [16], [20], [21]. Furthermore, user training is not mandatory for SSVEP-based BCI [22], [23]. In an SSVEP-based BCI, brain potentials are evoked with external stimuli, which can be flickering LEDs or flickering icons on a display. These brain signals do not depend on cognitive paths, thus being a useful communication channel also for people with cerebral diseases. Concerning the above discussion on hands-free AR, smart glasses LCD displays can be employed successfully for stimulus presentation.

In [24], research solutions are surveyed by highlighting that most state-of-the-art systems made use of two VEP-based paradigms, SSVEP or P300. It is also reported that video see-through technology is mostly considered, and that the main application field is robotics. However, there are still many limitations to the exploitation outside laboratories, such as motion artifacts [25], [26] and the trade-off between speed and performance of the BCI [27], especially when dry electrodes are employed. For this reason, recent works are still at the stage of feasibility studies [28], [29]. Although a comparison is not easy owing to differences in setups and applications, some examples of BCI-based systems for communication and control are reported here. In [30] a single-channel BCI employing high-frequency stimuli is proposed to build a speller. The user is stimulated for 10 s and the accuracy is 99.2%. Only 5 subjects were involved in the experiments, so that the usability of the system for different people cannot be estimated [31]. Another speller, exploiting a single-channel data acquisition with dry electrodes and deep neural networks for signal processing, was proposed in [32]. The accuracy was 97.4% with a stimulation time of 2 s, but only 8 subjects were considered in the experiments. A solution with AR glasses integrated with a BCI to control a quadcopter is reported in [28]. However, 14 dry electrodes and 2 reference electrodes were employed. The achieved accuracy was 85%,

*This work was supported by Universita' di Napoli Federico II and Politecnico di Torino.

[1]Department of Electrical Engineering and Information Technology (DIETI), Universita' degli Studi di Napoli Federico II.

[2]Department of Electronics and Telecommunications (DET), Politecnico di Torino.

0018-9456 (c) 2018 IEEE. Personal use is permitted, but republication/redistribution requires IEEE permission. See http://www.ieee.org/publications_standards/publications/rights/index.html for more information.

This article has been accepted for publication in a future issue of this journal, but has not been fully edited. Content may change prior to final publication. Citation information: DOI 10.1109/TIM.2019.2914712, IEEE Transactions on Instrumentation and Measurement

by considering 5 subjects executing a flight task.

In this paper, a monitoring system integrating AR glasses with BCI is proposed for applications in industrial inspection and maintenance. Main scientific aim is to increase simultaneously speed and accuracy of current SSVEP-based BCI single-channel instrumentation, in order to build a hands-free low-cost monitoring system, which is also wearable and non-invasive. Performance assessment was conducted on 20 subjects, in order to address the usability to a suitable group of people.

In particular, Section II details the architecture of the proposed AR-BCI system. Section III reports the physical design and the prototyping of the system, by proving its suitability for inspection aimed at maintenance in the framework of Industry 4.0 by a case study. Here, Bluetooth connectivity is exploited to communicate with a wireless sensor network [33], [34]. Finally, in Section IV, the metrological analysis of system performance mainly aimed at proving the decrease of real-time latency by simultaneously keeping accuracy as high as possible.

II. Proposal

A measurement instrument for wearable brain-computer interface is proposed for hands-free monitoring systems with augmented reality platform. The proposed AR-BCI system is employable in industrial inspection, where the user can communicate with wireless smart transducer networks and require the information for inspection without using hand, by merely starring at an icon.

In a traditional AR-based monitoring platform (Fig. 1a), data from a wireless sensor network are requested, received, and processed for industrial inspection. The user asks for data and their process results on the display by typical interfaces as touch-pads, vocal commands, or gestures.

In Industry 4.0, a novel human-machine interaction is needed with low cost, wearable, and hands-free features. In particular, at this aim, AR glasses have the advantage to be wearable. Most AR glasses allows to see both real and virtual scenes at once during the inspection, because their display is semi-transparent and semi-reflexive (optical see-through devices [4]).

A. Architecture

In the proposed monitoring system, the user input is replaced with a brain-computer interface, based on steady-state visually evoked potentials (SSVEP). SSVEP-based BCIs require visual stimulation, consisting here of flickering icons on the AR glasses display. On the AR glass display, flickering icons highlight the choices for the user during the industrial inspection task. Flickering aims to elicit an SSVEP in the occipital lobe of the user's brain. This neuronal activity is measured with an electroencephalography (EEG), and the acquired digital signal is transferred to the AR glasses microprocessor for elaboration. The result of this elaboration is a command associated to the user's intention (Fig. 1b). The AR glasses are employed for visual stimulation and for processing the brain signal acquired by an EEG-instrument. The user controls the system just starring at an icon insistently (e.g., for 2 s).

B. BCI instrument for AR input

In the architecture of Fig. 1b, the AR input interface is a non-invasive single-channel brain-computer interface. Only two dry electrodes are employed for differential acquisition of brain signals in order to build a highly wearable system. The electrodes are placed on the scalp, according to the 10-20 system [35] at the points "*Fpz*" and "*Oz*" highlighted in black in Fig. 2. This arises from the consideration that *"Oz"* is located in the occipital region of the brain associated to the visual activity, while *"Fpz"* is in a region without visual activity, i.e. the frontal region. Therefore, the differential acquisition aims to isolate the visual activity by subtracting the ongoing brain activity. A third passive electrode of ground is usually placed on the forehead, the ear, or even on a wrist or a leg [19]. This placement of only two active and dry electrodes makes the proposed AR-BCI instrument highly wearable in everyday-life applications.

The adopted BCI paradigm requires flickering icons on the AR glasses display for visual stimulation. The SSVEP oscillation, elicited when starring at a specific icon, is easily detected in the frequency domain. Thus, each icon blinks at a peculiar frequency. The user can input an option by just choosing the icon to stare at, and the choice is detected by assessing the corresponding frequency of the SSVEP oscillation. An amplitude modulation was not considered owing to inter-subject and intra-subject variability of SSVEP signals. A phase modulation would result in a more complex implementation of the stimuli. Therefore, these techniques would require further investigations, out of the scope of this work.

A simple power spectral density analysis is considered for brain signal processing. The aim is to guarantee low computational cost for implementation on a wearable device. Two main processing steps are carried out: *feature extraction* and *classification*. For *feature extraction*, a digital pass-band window-based FIR filter is first applied to the acquired signal. Then, zero-padding is applied prior to execute an FFT (Fast Fourier Transform). The power spectral density (PSD) analysis is carried out on the discrete amplitude spectrum of the brain signal. For each stimulus frequency f_1, the power in the corresponding bin k_1 is calculated as the sum of the squared amplitudes associated to k_1 and some nearest bins:

$$P(f_1) = \frac{1}{2k+1}\left[\sum_{n=k_1-k}^{k_1+k} A^2(n) + c\sum_{n=2k_1-k}^{2k_1+k} A^2(n)\right], \quad (1)$$

where k is the number of bins considered on the right and on the left of the bin k_1, and $A(n)$ the amplitude associated to the n-th bin. The amplitudes are obtained by dividing the FFT output by the number of samples. The second term in the squared parenthesis is related to the second harmonic of f_1, and c is a weighting factor for this harmonic. Higher-order harmonics are not considered owing to their poor SNR.

In the *classification*, for each stimulus frequency, the signal feature P is calculated and compared with a corresponding threshold th. If none of them is greater than the threshold, then the algorithm does not recognize any SSVEP. Conversely, the frequency f is detected as SSVEP oscillation. If more than

0018-9456 (c) 2018 IEEE. Personal use is permitted, but republication/redistribution requires IEEE permission. See http://www.ieee.org/publications_standards/publications/rights/index.html for more information.

This article has been accepted for publication in a future issue of this journal, but has not been fully edited. Content may change prior to final publication. Citation information: DOI 10.1109/TIM.2019.2914712, IEEE Transactions on Instrumentation and Measurement

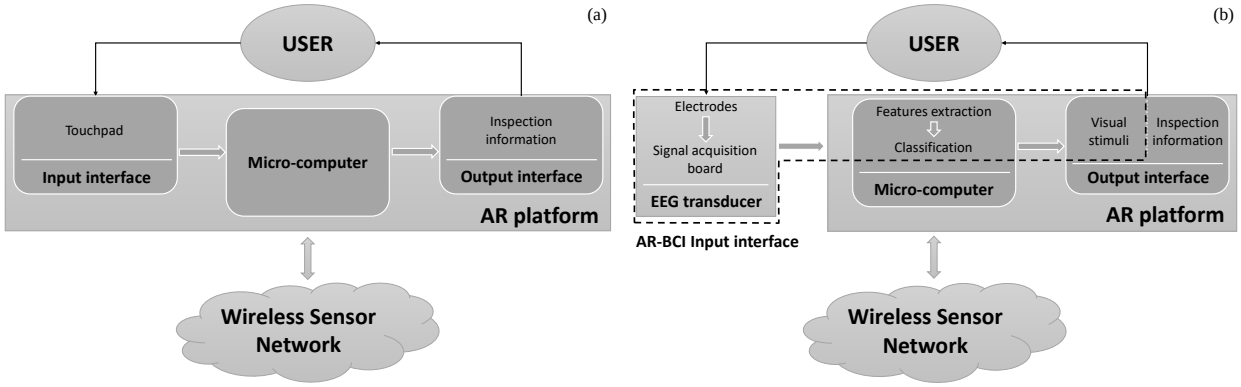

Figure 1: Architecture of an AR-based monitoring system, communicating with a wireless sensor network during industrial inspection: with input interface (a) traditional, and (b) brain computer-based.

one frequency is detected, the final result is associated to the greater value $P(f) - th(f)$.

The thresholds th were determined experimentally on human subjects by means of the method of the *Receiver Operating Characteristic* (ROC) [36]. For each subject, the thresholds corresponding to the stimulus frequencies, and the weighting factor c were identified by optimizing the classification accuracy. The accuracy in classifying N trials is defined as

$$A = \frac{tp + tn}{p + n}, \tag{2}$$

with p number of positives, n number of negatives ($N = p + n$), tp number of true positives, and tn number of true negatives. The resulting system requires minimal training of the algorithm (about 10 minutes) for the thresholds to be adapted to the specific final user.

III. Prototype

By referring to the architecture of Fig. 1b, the AR-BCI prototype exploits the *AR platform* Epson Moverio BT-200, with the related glasses as *Output interface*, and the Olimex EEG-SMT with dry electrodes as EEG transducer. An Android application runs on the *Micro-computer* Epson Moverio BT-200AR for processing brain signals in real time. The result is a low-cost wearable system, capable of communicating with external devices through Bluetooth. Information of interest for the user can be requested without using hands to a wireless sensor network. The SSVEP-based BCI exploits two icons, on opposite corners of the AR glasses screen, as stimulation to evoke potentials in the visual cortex. They substitute icons to be pressed on a classical touch-screen. These icons, instead, flicker in the *alpha* band [16], namely at nominal frequencies of 10.0 and 12.0 Hz, respectively. They were designed by means of the Android "open graphic library" (*openGL* [37]).

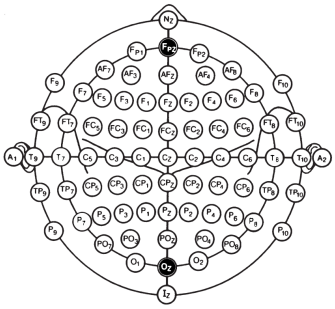

Figure 2: Placement of EEG electrodes in the International standard framework 10-20 [35] (in black): "*Fpz*" and "*Oz*", in the scalp frontal and occipital region, respectively.

The electrical brain activity is then acquired by means of the EEG transducer through a differential channel with two active electrodes and a grounding passive electrode. The active electrodes include a circuitry based on an operational amplifier for impedance matching. Wearability in daily use was improved by dry electrodes (i.e., without conductive gel). In this prototyping phase, a good electrical connection was ensured by a tight armband for the passive electrode on the left wrist, and a tight headband for the active electrodes on the user's scalp. Furthermore, silver pins were soldered to the active electrode placed at the occipital region of the scalp, in order to overcome the hair and contact the scalp directly [38].

The passive electrode provides a feedback for instrumentation amplifiers at the device input, while the two active electrodes are connected to the differential input of the instrumentation amplifier at the channel 1 (CH1). The overall gain from the signal pick-up to the analog-to-digital converter (ADC) of the transducer was set to be 6427 V/V. The input brain signal is also filtered analogically, and the overall pass-band is [0.16-59.00] Hz. A 10-bit resolution ADC provides the conversion, and the sampling frequency was set to 256.0 Sa/s. The digital signal is then transferred to the micro-computer of the AR platform for processing.

For the *feature extraction*, a window-based FIR filter was designed with MATLAB. The pass-band was set to [6-28] Hz, the filter order equal to 100, and the windowing is carried out with a Hamming. Thus, the harmonic content of interest, between 10.0 and 24.0 Hz (second harmonics of 12.0 Hz), is not corrupted. Simultaneously, the harmonic content in the stop band is attenuated at least by 50 dB, so that an eventual spectral leakage does not influence the frequencies of interest. Furthermore, the Hamming windowing aims to reduce the leakage at the frequencies of interest, while slightly

0018-9456 (c) 2018 IEEE. Personal use is permitted, but republication/redistribution requires IEEE permission. See http://www.ieee.org/publications_standards/publications/rights/index.html for more information.

This article has been accepted for publication in a future issue of this journal, but has not been fully edited. Content may change prior to final publication. Citation information: DOI 10.1109/TIM.2019.2914712, IEEE Transactions on Instrumentation and Measurement

loosing in spectral resolution. The pass-band was chosen also considering the need to reduce eye-blinking and muscle artifacts [39]. Indeed, linear filtering could be used to reduce noise introduced by artifacts, because other methods such as a regression method, need for a higher number of electrodes. Zero-padding follows: the number of zeros to append was chosen so that the total number of samples is the nearest power of 2. In addition, the zero-padded time windows were chosen to be a multiple of the period of 10.0 Hz and 12.0 Hz. Thus, there is always a bin in the discrete spectrum corresponding to 0.100 or 0.083 s (10.0 or 12.0 Hz). The number of bins for the calculation of $P(f)$, eq. (1), is such that the frequency neighborhood equals 0.4 Hz, with the further constraint that at least one bin on the left and one on the right of the frequency of interest must be considered. Moreover, the actual flickering frequency can slightly differ from the nominal value (Fig. 3). Therefore, the bin corresponding to the frequency of interest is preventively found in the neighborhood of the nominal frequency looking for the maximum amplitude. This neighborhood is, again, equal to 0.4 Hz.

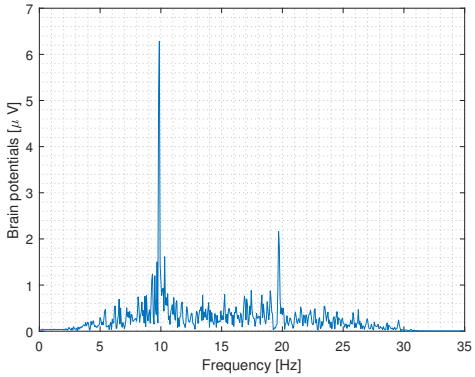

Figure 3: Spectrum of an SSVEP signal acquired for 10.0 s, after filtering and zero-padding to 16 s (the peak is about at 10 Hz).

A. Case Study

The possibility of employing successfully the proposed instrument in a hands-free inspection task for Industry 4.0 was proven experimentally. Main scenario consists of a technician inspecting visually a complex industrial plant by looking at its composing parts, like electrical machines, cables, power drives, and so on. The plant is equipped by a distributed measurement system with several wireless smart transducers for real-time monitoring and advanced diagnostics.

For this case study, a prototype was developed with the Bluetooth protocol for communication between the AR glasses and the monitoring system. The modified Android application searches automatically for the Bluetooth smart transducers associated with the AR glasses. Once found, the closest transducers with highest Bluetooth signal are made accessible and displayed on the AR glass display (Fig. 4). The user is prompted to select the transducer and then to connect. Once connected, the transducer answers by sending the measured

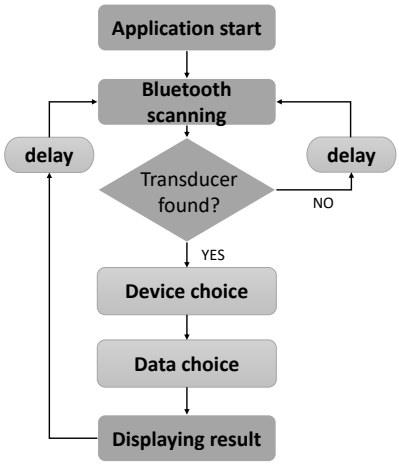

Figure 4: Android application diagram for inspection task in Industry 4.0 framework: smart transducers and related measurements are selected by starring at flickering icons.

quantities, and finally the user can choose the result of the specific quantity to be displayed. The commands are sent to the transducer without the use of hands, just starring at the corresponding icon.

Fig. 5 shows an user wearing a prototype of the AR-BCI system during an emulated inspection task of temperature and humidity. To input a selection in a menu (Fig. 6), the

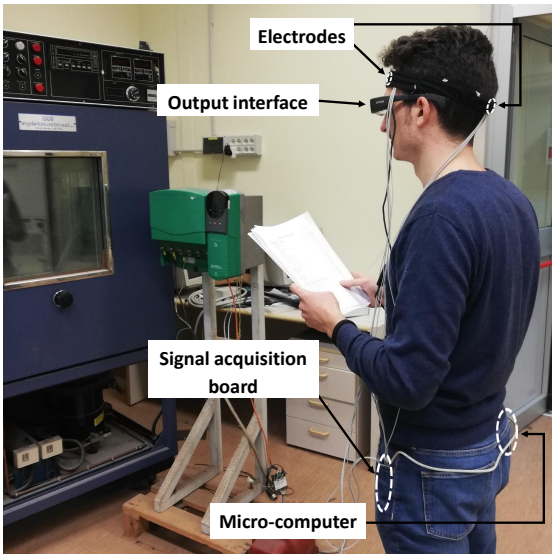

Figure 5: A user wearing the AR-BCI system during an inspection task.

user stares at a flickering icon and, after few seconds, the corresponding command is sent. Specifically, the user input is obtained by the stimulus of the flickering white square corresponding to the gazed icon. In AR glasses, actual background image is blurred to put focus on the selection. In this straightforward proof-of-principle application, the possible commands correspond to the result of the SSVEP classification: "*Temperature*" and "*Humidity*". If the brain signal is not recognized, the user is prompted to repeat the choice.

0018-9456 (c) 2018 IEEE. Personal use is permitted, but republication/redistribution requires IEEE permission. See http://www.ieee.org/publications_standards/publications/rights/index.html for more information.

This article has been accepted for publication in a future issue of this journal, but has not been fully edited. Content may change prior to final publication. Citation information: DOI 10.1109/TIM.2019.2914712, IEEE Transactions on Instrumentation and Measurement

Thus, the AR-BCI system allows to access measurement data relevant to the specific area under inspection without engaging the user hands. The user has hands free to hold documentation or reference gears while requesting data from transducers.

IV. Experimental Results

In this section, the results of the experimental campaign for optimizing the real-time metrological performance of the BCI instrument are reported. In particular, the main aim was to characterize the measurement system in order to maximize the SSVEP classification accuracy, by simultaneously minimizing time, i.e. latency. The trade-off between accuracy and latency is essential in a typical application of inspection under the framework of Industry 4.0.

In the following, (i) the *experimental setup*, (ii) the *thresholds determination*, (iii) the *configuration optimization*, and (iv) the *prototype validation* are detailed.

A. Experimental setup

Twenty subjects, 13 males and 7 females between 22 and 47 years old, took part to the experiments. Experiments were conducted in laboratory with artificial illumination. The window was closed to avoid any sunlight presence, while the background luminous emittance resulting from neon lights was measured to be (97 $\pm$ 2) lx. Each subject under test was asked to seat on a comfortable chair with armrest and limit the unnecessary movements, such as moving the head or the arm. This was necessary in the first phase to avoid motion artifacts in order to check for the correct electrodes positioning. Then, he/she wore the AR glasses, a tight armband and a tight headband. The signal acquisition board of the EEG transducer was then connected to a laptop, where a MATLAB application was running. The laptop was disconnected from the AC power before connecting this transducer. At the beginning of each test, the EEG signal amplitude was checked through BrainBay [40], an open-source software for displaying on line EEG data (Fig. 7). A specific sequence was adopted for connecting the electrodes.

- The passive electrode was connected to the input Drive Right Leg (DRL) and applied on the subject left wrist with the armband. The acquired signal was null at this moment, owing to the absence of signal at CH1.
- The active electrode without silver pins was connected to the negative terminal of the channel 1 (CH1) and applied at the point "*Fpz*" (frontal lobe of the scalp) with the help of the headband.
- After a transient of few seconds, the acquired signal had to be zero again, because CH1 is still an open circuit at this moment, and the internal circuitry reaches a stationary condition with a null output.
- Last, the active electrode with silver pins was connected to the positive terminal CH1 and applied at "Oz" (occipital region of the scalp) with the help of the headband. After few seconds, the stationary condition should be characterized by oscillations with a peak-to-peak amplitude below 100 μV, while some artifacts can be present corresponding to the subject's eyes blinking.

Figure 6: Example of an inspection task: measure selection menu, with flickering white squares for options (as usual in AR glasses, background image is blurred to focus on the selection).

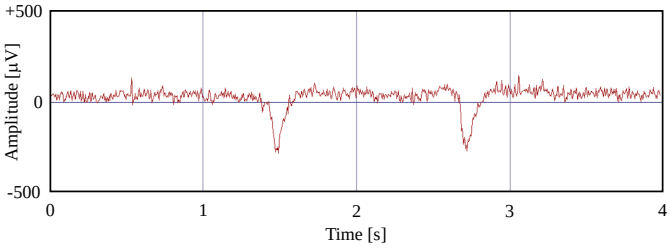

Figure 7: Example of a single-channel electroencephalogram acquired with BrainBay: two artifacts from eyes blinking are present (valleys).

For a correct application of the electrodes, hair has to be avoided on the wrist and in the frontal region of the scalp. Furthermore, for the silver pins, hair is to be overcome in the occipital region of the scalp. A stable contact of the electrodes with the skin is ensured by tight bands, provided that an excess could introduce artifacts due to the heart beat." A typical signal measured after wearing the EEG-SMT transducer is represented in Fig. 7. Then, the signal was analyzed in the frequency domain in absence of visual stimulation. Fig. 8 shows a typical spectrum in this condition.

B. Threshold determination

The test campaign was aimed initially to identify the thresholds th_{10} and th_{12} associated to stimulation at 10.0 Hz and 12.0 Hz, respectively. These thresholds are associated to the power spectral density of the brain signals. The combination factor c of first and second harmonic in eq. (1) was identified too. Due to the different neurophysiological characteristics of each subject, an inter-subject variation was expected. Thus, the identification phase corresponds to the training necessary for the algorithm to be customized to the user before the use. This lasts less than 10 minutes, namely the time needed to carry out the trials described in the following experimental procedure. Thanks to this phase, the SSVEP classification is adapted to the specific user with minimal training of the algorithm.

1) Experimental procedure: For each subject, 24 trials with two flickering icons were first conducted. In each trial,

0018-9456 (c) 2018 IEEE. Personal use is permitted, but republication/redistribution requires IEEE permission. See http://www.ieee.org/publications_standards/publications/rights/index.html for more information.

This article has been accepted for publication in a future issue of this journal, but has not been fully edited. Content may change prior to final publication. Citation information: DOI 10.1109/TIM.2019.2914712, IEEE Transactions on Instrumentation and Measurement

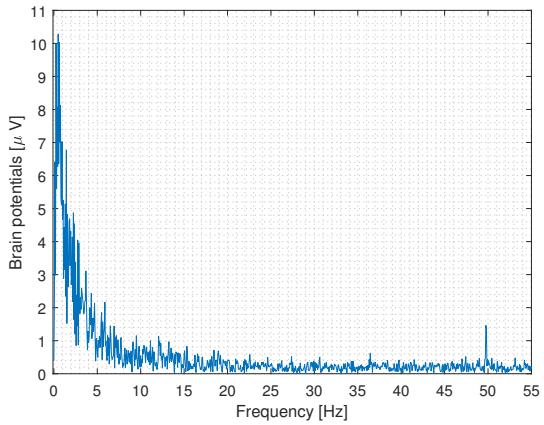

Figure 8: Typical noise floor when the EEG-SMT setup is completed and the user is not stimulated (without digital filtering).

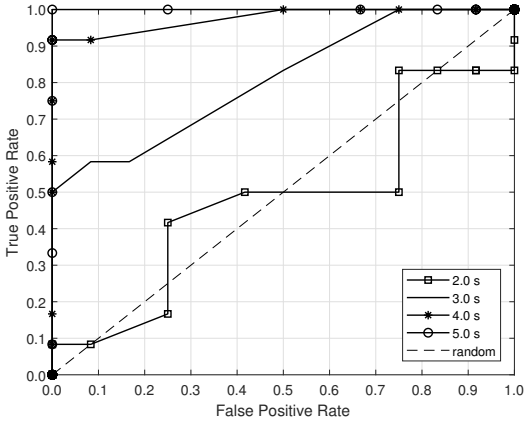

Figure 9: ROC curves for the binary classifier "frequency 10.0 Hz?", for the 24 trials of the subject "*CraSim*" (c=2, with four time windows).

the brain signal acquisition lasted 10.0 s, with few seconds between consecutive trials. The subject under test could arbitrarily chose the icon to stare at. The only constraint was that the subject had to choose 12 times 10.0 Hz and 12 times 12.0 Hz. Then, the subject had to declare the choice. The MATLAB post-processing did not allow to synchronize stimulation and acquisition. Therefore, as the subject under test started a stimulation, he/she had to say "go" for the tester to start the 10.0 s acquisition.

2) Data analysis: The brain signals acquired during the experimental campaign were elaborated calculating the signal feature $P(f)$ of eq. (1) for 10.0 Hz and 12.0 Hz after the pre-processing described previously. For each stimulus frequency, a binary classifier was trained exploiting the "Receiver Operating Characteristic" (ROC) curve and the label associated to each signal [36]. The classifier "is the frequency f?" returns "true" when $P(f) > th(f)$, and "false" otherwise. Fig. 9 reports an example of ROC curve for the 10.0 Hz binary classifier, considering the 24 trials of a single subject. The different time windows are obtained in post-processing considering fewer samples of each signal acquired for 10.0 s. The optimal threshold is identified as the point of the curve with 12 true positives (the maximum) and the minimum number of false positives. This aims to guarantee that each classifiers correctly classifies all the true positives. Meanwhile, the possible false positives should be "blocked" in the comparison with the result of the other classifier. In the example of Fig. 9, the point (0,1) belongs to the ROC curve plotted for 5 s. It corresponds to no false positives, and all true positives. Hence, the considered 10.0 Hz binary classifier is a perfect classifier when the time window is 5 s. Instead, for smaller time windows, the classifier is not perfect.

The identification phase exploits the ROC curve method for seven time window values: 10.0 s, 8.0 s, 6.0 s, 5.0 s, 4.0 s, 3.0 s, 2.0 s. For each of them, the optimal th_{10} and th_{12} are meant to maximize the classification accuracy. The identification phase is summarized on the left of Fig. 10, along with the validation steps described in the following

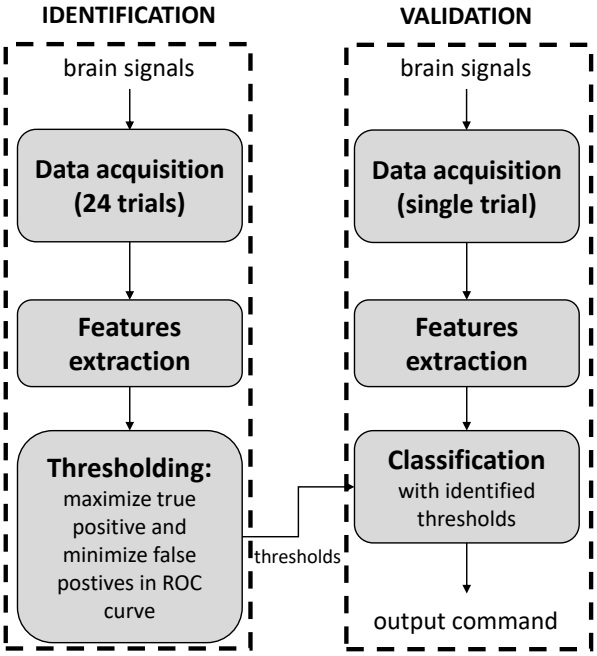

Figure 10: Flow diagram of the identification and validation.

(on the right). The results of the algorithm also depend on the combination factor c between first and second harmonic. Hence, the exposed procedure was repeated for c = [0 1 2 3 4 5 6]. The optimal value of c can depend on the considered time window. For each value of the time window, c is found considering the accuracy closest to the 100%. The robustness of the result was also evaluated considering if the same value of accuracy is obtained for consecutive values of c, and the final c is chosen as the mean one.

3) Identification results: The results of the identification test campaign are reported in Tab. I. The identified values of c span from 0 to 6 depending on the subject and more weakly on time windows. The thresholds vary from 0.1 μV^2 up to 10.0 μV^2 and strongly depend on the considered time window and the subject. The overall average accuracy on all

0018-9456 (c) 2018 IEEE. Personal use is permitted, but republication/redistribution requires IEEE permission. See http://www.ieee.org/publications_standards/publications/rights/index.html for more information.

This article has been accepted for publication in a future issue of this journal, but has not been fully edited. Content may change prior to final publication. Citation information: DOI 10.1109/TIM.2019.2914712, IEEE Transactions on Instrumentation and Measurement

subjects was also assessed as a function of latency. In the table, the minimum time window for 100.0% accuracy, varying from above 10.0 s down to 2.0 s, is highlighted. The subjects "*EspAnt*", "*MocNic*" and "*DeAGio*" had already experience with SSVEP-based BCI, while all the other candidates had no experience with BCIs. The performance reached by "*EspAnt*" could be explained with an SSVEP generation attitude due to his previous experience. However, similar performance are reached also by subjects without experience, notably "*DeLAnn*". In principle, subjects with long and/or wavy hair affecting electrodes application should be in disadvantage. However, the experimental results did not show any evidence of that. The better four in terms of accuracy versus latency, for example, have both long and short hair cut. A wrongly classified signal corresponds to an accuracy diminishing of about 4.2%. This value corresponds to the resolution dictated by the number of trails conducted for each subject, namely one trial over the total 24. Hence, the values reported in Tab. I are given with this resolution.

During the identification campaign, two subjects were considered as outliers because their brain signals had amplitudes lower than the average. The mean amplitude was estimated considering the twenty subjects reported in the table. The reason was led back to their accentuated myopia (at least minus 3 dioptres). Few subjects had normal or corrected to normal vision. Due to the AR glasses, subject could correct an eventual deficit visus only with contact lenses. In the other cases, they suffered from myopia, but with less than minus 3 dioptres.

Even with a single channel and a simple signal processing, accuracy of 98.9% was achieved with a latency of 10.0 s, dropping to 81.1% at 2.0 s. The usual trend is an accuracy diminishing when fewer samples are considered for the signal. However, some exceptions are present for the subjects "*MocNic*" at 8.0 s, "*ErrErn*" at 2.0 s, "*PesMar*" at 4.0 s, and "*CicMel*" at 5.0 s and 2.0 s. This could be explained with a varying attention of the user during the stimulation time, so that a longer time window is not necessarily better than a short one. Nonetheless, this could be solved with a more sophisticated algorithm.

C. Configuration optimization

A further experimental test campaign was carried out for validating the achieved threshold results by using the integrated AR-BCI system. After the qualitative checks on BrainBay, the results of the identification phase had to be validated with further trials, by connecting the EEG transducer directly to the AR glasses. The validation test campaign consisted in the use of the final AR-BCI system for the communication with external devices through Bluetooth. Starring at an icon, the subject could arbitrarily choose the command to actuate during the communication, with the constraint that he/she had to choose 12 times the command associated to the 10.0 Hz flickering icon, and 12 times the command associated to 12.0 Hz. For each user, the stimulation time was set to the minimum latency that resulted in 100% accuracy during identification (first 24 trials) and to 10.0 s (last 24 trials). If the minimum latency resulted greater than 5 s, the first trials were conducted setting a 5 s stimulation. This value was considered as an acceptable latency for using the AR-BCI system in industrial applications. During validation, the signals are processed as described in the preceding sections, but the algorithm was implemented in Android. The identified parameters associated to the respective time windows, namely th_{12}, th_{10}, and c, were set in the algorithm as well as the stimulation time. The accuracy obtained during validation was assessed thanks to a feedback from the user about the successful or unsuccessful command choice. Hence, this setup slightly differed from the identification experimental setup because the laptop was not employed, the EEG transducer supply came directly from the AR glasses battery, and the user had to conduct an emulated industrial task. Brain signals were also recorded for further post-processing.

D. Prototype validation

The validation results are reported in Tab. II. The mean accuracies drop by about 20% both for the minimum latency and for 10.0 s. However, a significant inter-subject variability is experimented, and for some subjects, the accuracy is drastically lower than during identification. The validation setup has few differences with respect to the identification. Even though the subjects had to use the Android application of Subsection III-A, the flickering icon were presented on a black screen as in preceding tests. However, the subjects complained about a greater difficulty in being focused on a visual stimulus with respect to the preceding phase. This was led back to two main factors, (i) the need for focus on an icon while conducting an inspection task, and (ii) the need to stare at the icon before the flickering started, thus having to maintain the focus for more time. In particular, in the current Android application, the available selections appear 4 s before the flickering start, and the user usually starts starring at the icon as far as it appears. This last hypothesis is corroborated with the fact that some subjects reached an accuracy at 10 s lower than the one at the minimum latency. Indeed, the need to emulate an industrial task changed the experimental conditions, due to a different emotional state for the user. While in the first experiments the user could be relaxed when starring at an icon, the industrial task to carry on in the second phase required higher attention, thus influencing the brain signals to be measured. In principle, a longer stimulation should lead to a more clear SSVEP signal, but this is true only if the subject maintains the focus on the icon. Another hypothesis is that the identified thresholds guarantee a correct classification during validation only for some subjects. Nonetheless, the robustness of the thresholds could not be evaluated *a priori*. The confirmation of that requires a more complex signal analysis, with particular reference to the data acquired during validation. In addition, the check of correct application of electrodes would be important when using the integrated wearable system. These improvements are addressed to a next work. At the present state, the validation results are influenced by a problem in the system setup reproducibility. Finally, the contribution of this work is highlighted in Tab. III by comparison with works in the SSVEP-BCI field.

0018-9456 (c) 2018 IEEE. Personal use is permitted, but republication/redistribution requires IEEE permission. See http://www.ieee.org/publications_standards/publications/rights/index.html for more information.

This article has been accepted for publication in a future issue of this journal, but has not been fully edited. Content may change prior to final publication. Citation information: DOI 10.1109/TIM.2019.2914712, IEEE Transactions on Instrumentation and Measurement

Subject	10.0 s	8.0 s	6.0 s	5.0 s	4.0 s	3.0 s	2.0 s
DeLAnn	100.0%	100.0%	100.0%	100.0%	100.0%	100.0%	100.0%
EspAnt	100.0%	100.0%	100.0%	100.0%	100.0%	100.0%	100.0%
CioAnt	100.0%	100.0%	100.0%	100.0%	100.0%	100.0%	95.8%
PasLor	100.0%	100.0%	100.0%	100.0%	100.0%	100.0%	95.8%
CraFed	100.0%	100.0%	100.0%	100.0%	100.0%	100.0%	87.5%
DasCre	100.0%	100.0%	100.0%	100.0%	100.0%	95.8%	91.7%
CapFra	100.0%	100.0%	100.0%	100.0%	100.0%	95.8%	91.7%
FalGia	100.0%	100.0%	100.0%	100.0%	100.0%	95.8%	87.5%
MocNic	100.0%	95.8%	100.0%	100.0%	100.0%	91.7%	87.5%
ErrErn	100.0%	100.0%	100.0%	100.0%	91.6%	91.7%	95.8%
CraSim	100.0%	100.0%	100.0%	100.0%	95.8%	79.2%	54.2%
TeoAle	100.0%	100.0%	100.0%	95.8%	95.8%	83.3%	75.0%
PetPas	100.0%	100.0%	100.0%	95.8%	95.8%	70.8%	50.0%
PesMar	100.0%	100.0%	95.8%	95.8%	100.0%	95.8%	95.8%
DeAGio	100.0%	95.8%	95.8%	91.7%	83.3%	83.3%	83.3%
CanAle	100.0%	95.8%	95.8%	91.7%	87.5%	83.3%	66.7%
FroMir	95.8%	95.8%	95.8%	95.8%	91.7%	75.0%	70.8%
VasBen	95.8%	95.8%	87.5%	83.3%	83.3%	75.0%	75.0%
SpeMar	95.8%	95.8%	91.7%	91.7%	87.5%	62.5%	45.8%
CicMel	91.7%	87.5%	87.5%	79.2%	87.5%	75.0%	83.3%
MEAN	98.9%	98.1%	97.5%	96.0%	94.8%	87.9%	81.1%

Table I: Classification accuracy of SSVEP signals for each subject and mean accuracy at varying time window (100% accuracy for a minimum time window underlined). All the reported values have an accuracy equal to 4.2%.

Subject	Accuracy at 10 s	Accuracy at min	Minimum latency (s)
DeLAnn	83.3%	87.5%	2.0
EspAnt	100.0%	95.8%	2.0
CioAnt	83.3%	95.8%	3.0
PasLor	95.8%	70.8%	3.0
CraFed	83.3%	83.3%	3.0
DasCre	91.7%	95.8%	4.0
CapFra	83.3%	91.7%	4.0
FalGia	70.8%	75.0%	4.0
MocNic	95.8%	70.8%	4.0
ErrErn	62.5%	95.8%	5.0
CraSim	75.0%	70.8%	5.0
TeoAle	91.7%	79.2%	-
PetPas	95.8%	66.7%	-
PesMar	83.3%	87.5%	-
DeAGio	87.5%	70.8%	-
CanAle	58.3%	70.8%	-
FroMir	79.2%	75.0%	-
VasBen	66.7%	50.0%	-
SpeMar	66.7%	91.7%	-
CicMel	79.2%	70.8%	-
MEAN	81.6%	75.4%	

Table II: Classification accuracy of SSVEP signals when using the AR-BCI system for an inspection task (time window: 10.0 s, minimum latency, or 5 s; and "-": subjects with a minimum latency greater than 5 s.

V. Conclusions

A system, integrating augmented reality glasses with a non-invasive single-channel brain-computer interface based on SSVEP, is proposed for application in Industry 4.0. This work focuses on the BCI instrument for measuring the AR input directly by the user EEG. The user can carry out inspection tasks, receiving data from external wireless smart transducer networks, with hands free for other concomitant tasks. An experimental metrological characterization was carried out to assess and optimize the real-time metrological performance of the system. Further validation experiments were conducted in an emulated inspection task of a case study of Industry 4.0.

The experimental results demonstrate that the minimum stimulation and acquisition time for the SSVEP signals in a single-channel BCI can be as low as 2.0 s with accuracy up to 90.0% - 100.0% for some subjects. The average accuracy was found to be 81.1% at 2.0 s, and grows up to 98.9% at 10.0 s. The proposed system was tested only on healthy subjects. However, future tests will be devoted to subjects with brain disease or anomalies, in order to explore limitations in usefulness and competency. A lightweight processing relying on data from a single channel would be needed to keep the capability of an on-line analysis. Further future research will deal with the optimization of visual stimuli parameters to reduce eye fatigue and increase the user focus. In future work, the use of neuro-feedback can improve the accuracy, reduce the latency, and support a quick focus. As an example, detecting an increase in power in the first fractions of second in one of the PSD bins can be used to reduce the brightness of the remaining icons.

Acknowledgments

The authors thank A. Cioffi for her support during the experimental campaign. This paper is dedicated to the memory of the late profs. Massimo D'Apuzzo and Domenico Grimaldi.

References

[1] R. T. Azuma, "A survey of augmented reality," *Presence: Teleoperators & Virtual Environments*, vol. 6, no. 4, pp. 355–385, 1997.

[2] R. Azuma, Y. Baillot, R. Behringer, S. Feiner, S. Julier, and B. MacIntyre, "Recent advances in augmented reality," tech. rep., NAVAL RESEARCH LAB WASHINGTON DC, 2001.

[3] A. Alamri, J. Cha, and A. El Saddik, "AR-REHAB: An augmented reality framework for poststroke-patient rehabilitation," *IEEE Transactions on Instrumentation and Measurement*, vol. 59, no. 10, pp. 2554–2563, 2010.

[4] D. Chatzopoulos, C. Bermejo, Z. Huang, and P. Hui, "Mobile augmented reality survey: From where we are to where we go," *IEEE Access*, vol. 5, pp. 6917–6950, 2017.

[5] M. Rüßmann, M. Lorenz, P. Gerbert, M. Waldner, J. Justus, P. Engel, and M. Harnisch, "Industry 4.0: The future of productivity and growth in manufacturing industries," *Boston Consulting Group*, vol. 9, 2015.

0018-9456 (c) 2018 IEEE. Personal use is permitted, but republication/redistribution requires IEEE permission. See http://www.ieee.org/publications_standards/publications/rights/index.html for more information.

This article has been accepted for publication in a future issue of this journal, but has not been fully edited. Content may change prior to final publication. Citation information: DOI 10.1109/TIM.2019.2914712, IEEE Transactions on Instrumentation and Measurement

	low cost	wearability	trainingless	participants	accuracy/latency
P. Kaczmarek et al. [41] 2015	✓	✗	✗	4	76%/2 s
P.M.S. Prasad et al. [42] 2017	n.a.	✓	✗	5	94%/2 s
Y. Wei et al. [42] 2017	✓	✗	✗	10	92%/4 s
S. Ajami et al. [30] 2018	n.a.	∼	✓	5	99.2%/10 s
M. Wang et al. [28] 2018	✓	✓	✓	10 5	78%/ 5 s 85%/ 5 s
our previous paper [23] 2018	✓	✓	✓	10	90%/10 s
T.-H. Nguyen et al. [32] 2019	∼	∼	✗	8	97.4%/ 2 s
our current paper (training) 2019	✓	✓	∼	20	98.9%/10 s 81.1%/2 s
our current paper (validation) 2019	✓	✓	∼	20	81.6%/10 s 75.4%/ $\leq$ 5 s

Table III: Comparison of recent research solutions on SSVEP-based BCIs for communication and control.

[6] M. Rüßmann, M. Lorenz, P. Gerbert, M. Waldner, J. Justus, P. Engel, and M. Harnisch, "Industry 4.0: The future of productivity and growth in manufacturing industries." https://bcg.com/publications/2015/engineered_products_project_business_industry_4_future_productivity_growth_manufacturing_industries.aspx, 2015.

[7] N. Gavish, T. Gutiérrez, S. Webel, J. Rodríguez, M. Peveri, U. Bockholt, and F. Tecchia, "Evaluating virtual reality and augmented reality training for industrial maintenance and assembly tasks," *Interactive Learning Environments*, vol. 23, no. 6, pp. 778–798, 2015.

[8] H.-C. Yan, J.-H. Zhou, and C. K. Pang, "Machinery degradation inspection and maintenance using a cost-optimal non-fixed periodic strategy," *IEEE Transactions on Instrumentation and Measurement*, vol. 65, no. 9, pp. 2067–2077, 2016.

[9] R. Palmarini, J. A. Erkoyuncu, R. Roy, and H. Torabmostaedi, "A systematic review of augmented reality applications in maintenance," *Robotics and Computer-Integrated Manufacturing*, vol. 49, pp. 215–228, 2018.

[10] J. R. Wolpaw, N. Birbaumer, W. J. Heetderks, D. J. McFarland, P. H. Peckham, G. Schalk, E. Donchin, L. A. Quatrano, C. J. Robinson, and T. M. Vaughan, "Brain-computer interface technology: a review of the first international meeting," *IEEE transactions on rehabilitation engineering*, vol. 8, no. 2, pp. 164–173, 2000.

[11] G. Schalk, D. J. McFarland, T. Hinterberger, N. Birbaumer, and J. R. Wolpaw, "BCI2000: a general-purpose brain-computer interface (BCI) system," *IEEE Transactions on biomedical engineering*, vol. 51, no. 6, pp. 1034–1043, 2004.

[12] M. Ahn and S. C. Jun, "Performance variation in motor imagery brain–computer interface: a brief review," *Journal of neuroscience methods*, vol. 243, pp. 103–110, 2015.

[13] C.-C. Lo, T.-Y. Chien, Y.-C. Chen, S.-H. Tsai, W.-C. Fang, and B.-S. Lin, "A wearable channel selection-based brain-computer interface for motor imagery detection," *Sensors*, vol. 16, no. 2, p. 213, 2016.

[14] T. O. Zander and C. Kothe, "Towards passive brain–computer interfaces: applying brain–computer interface technology to human–machine systems in general," *Journal of neural engineering*, vol. 8, no. 2, p. 025005, 2011.

[15] C. Guger, S. Daban, E. Sellers, C. Holzner, G. Krausz, R. Carabalona, F. Gramatica, and G. Edlinger, "How many people are able to control a P300-based brain–computer interface (BCI)?," *Neuroscience letters*, vol. 462, no. 1, pp. 94–98, 2009.

[16] Y. Wang, R. Wang, X. Gao, B. Hong, and S. Gao, "A practical VEP-based brain-computer interface," *IEEE Transactions on Neural Systems and Rehabilitation Engineering*, vol. 14, no. 2, pp. 234–240, 2006.

[17] S. Ajami, A. Mahnam, and V. Abootalebi, "Development of a practical high frequency brain–computer interface based on steady-state visual evoked potentials using a single channel of EEG," *Biocybernetics and Biomedical Engineering*, vol. 38, no. 1, pp. 106–114, 2018.

[18] Y.-T. Wang, Y. Wang, and T.-P. Jung, "A cell-phone-based brain–computer interface for communication in daily life," *Journal of neural engineering*, vol. 8, no. 2, p. 025018, 2011.

[19] M. Teplan *et al.*, "Fundamentals of EEG measurement," *Measurement science review*, vol. 2, no. 2, pp. 1–11, 2002.

[20] M. Cheng, X. Gao, S. Gao, and D. Xu, "Design and implementation of a brain-computer interface with high transfer rates," *IEEE transactions on biomedical engineering*, vol. 49, no. 10, pp. 1181–1186, 2002.

[21] I. Volosyak, F. Gembler, and P. Stawicki, "Age-related differences in SSVEP-based BCI performance," *Neurocomputing*, vol. 250, pp. 57–64, 2017.

[22] H. Cecotti, "A self-paced and calibration-less SSVEP-based brain–computer interface speller," *IEEE Transactions on Neural Systems and Rehabilitation Engineering*, vol. 18, no. 2, pp. 127–133, 2010.

[23] L. Angrisani, P. Arpaia, D. Casinelli, and N. Moccaldi, "A single-channel ssvep-based instrument with off-the-shelf components for trainingless brain-computer interfaces," *IEEE Transactions on Instrumentation and Measurement*, 2018.

[24] H. Si-Mohammed, F. Argelaguet, G. Casiez, N. Roussel, and A. Lécuyer, "Brain-computer interfaces and augmented reality: A state of the art," in *Graz Brain-Computer Interface Conference*, 2017.

[25] J. Penders, "Wearable, wireless eeg solutions in daily life applications: What are we missing?," *IEEE Journal of Biomedical and Health Informatics*, vol. 19, pp. 6–21, 2015.

[26] J. Minguillon, M. A. Lopez-Gordo, and F. Pelayo, "Trends in eeg-bci for daily-life: Requirements for artifact removal," *Biomedical Signal Processing and Control*, vol. 31, pp. 407–418, 2017.

[27] M. Spüler, "A high-speed brain-computer interface (BCI) using dry EEG electrodes," *PloS one*, vol. 12, no. 2, p. e0172400, 2017.

[28] M. Wang, R. Li, R. Zhang, G. Li, and D. Zhang, "A Wearable SSVEP-Based BCI System for Quadcopter Control Using Head-Mounted Device," *IEEE Access*, vol. 6, pp. 26789–26798, 2018.

[29] H. Si-Mohammed, J. Petit, C. Jeunet, F. Argelaguet, F. Spindler, A. Évain, N. Roussel, G. Casiez, and A. Lécuyer, "Towards bci-based interfaces for augmented reality: Feasibility, design and evaluation," *IEEE transactions on visualization and computer graphics*, 2018.

[30] S. Ajami, A. Mahnam, and V. Abootalebi, "Development of a practical high frequency brain–computer interface based on steady-state visual evoked potentials using a single channel of EEG," *Biocybernetics and Biomedical Engineering*, vol. 38, no. 1, pp. 106–114, 2018.

[31] C. Guger, B. Z. Allison, B. Großwindhager, R. Prückl, C. Hintermüller, C. Kapeller, M. Bruckner, G. Krausz, and G. Edlinger, "How many people could use an SSVEP BCI?," *Frontiers in neuroscience*, vol. 6, p. 169, 2012.

[32] T.-H. Nguyen and W.-Y. Chung, "A Single-Channel SSVEP-Based BCI Speller Using Deep Learning," *IEEE Access*, vol. 7, pp. 1752–1763, 2019.

[33] G. Mois, S. Folea, and T. Sanislav, "Analysis of three iot-based wireless sensors for environmental monitoring," *IEEE Transactions on Instrumentation and Measurement*, vol. 66, no. 8, pp. 2056–2064, 2017.

[34] L. Lombardo, S. Corbellini, M. Parvis, A. Elsayed, E. Angelini, and S. Grassini, "Wireless sensor network for distributed environmental monitoring," *IEEE Transactions on Instrumentation and Measurement*, vol. 67, no. 5, pp. 1214–1222, 2018.

[35] G. H. Klem, H. O. Lüders, H. Jasper, C. Elger, *et al.*, "The ten-twenty electrode system of the international federation," *Electroencephalogr Clin Neurophysiol*, vol. 52, no. 3, pp. 3–6, 1999.

0018-9456 (c) 2018 IEEE. Personal use is permitted, but republication/redistribution requires IEEE permission. See http://www.ieee.org/publications_standards/publications/rights/index.html for more information.

This article has been accepted for publication in a future issue of this journal, but has not been fully edited. Content may change prior to final publication. Citation information: DOI 10.1109/TIM.2019.2914712, IEEE Transactions on Instrumentation and Measurement

[36] S. H. Park, J. M. Goo, and C.-H. Jo, "Receiver operating characteristic (roc) curve: practical review for radiologists," *Korean Journal of Radiology*, vol. 5, no. 1, pp. 11–18, 2004.

[37] M. Segal and K. Akeley, "The OpenGL Graphics System: A Specification (Version 4.0, Core Profile)." https://www.khronos.org/registry/OpenGL/specs/gl/glspec40.core.pdf, 2010.

[38] Y. M. Chi, Y.-T. Wang, Y. Wang, C. Maier, T.-P. Jung, and G. Cauwenberghs, "Dry and noncontact EEG sensors for mobile brain–computer interfaces," *IEEE Transactions on Neural Systems and Rehabilitation Engineering*, vol. 20, no. 2, pp. 228–235, 2012.

[39] M. Fatourechi, A. Bashashati, R. K. Ward, and G. E. Birch, "EMG and EOG artifacts in brain computer interface systems: A survey," *Clinical neurophysiology*, vol. 118, no. 3, pp. 480–494, 2007.

[40] "BrainBay - an OpenSource Biosignal project." http://www.shifz.org/brainbay/.

[41] P. Kaczmarek and P. Salomon, "Towards ssvep-based, portable, responsive brain-computer interface," in *2015 37th Annual International Conference of the IEEE Engineering in Medicine and Biology Society (EMBC)*, pp. 1095–1098, IEEE, 2015.

[42] P. S. Prasad, R. Swarnkar, K. V. Prasad, M. Radhakrishnan, M. F. Hashmi, and A. Keskar, "Ssvep signal detection for bci application," in *2017 IEEE 7th International Advance Computing Conference (IACC)*, pp. 590–595, IEEE, 2017.

0018-9456 (c) 2018 IEEE. Personal use is permitted, but republication/redistribution requires IEEE permission. See http://www.ieee.org/publications_standards/publications/rights/index.html for more information.